Science Translational Medicine
AAAS

www.sciencetranslationalmedicine.org/cgi/content/full/10/461/eaat1445/DC1

Supplementary Materials for

p95HER2–T cell bispecific antibody for breast cancer treatment

Irene Rius Ruiz, Rocio Vicario, Beatriz Morancho, Cristina Bernadó Morales, Enrique J. Arenas, Sylvia Herter, Anne Freimoser-Grundschober, Jitka Somandin, Johannes Sam, Oliver Ast, Águeda Martinez Barriocanal, Antonio Luque, Marta Escorihuela, Ismael Varela, Isabel Cuartas, Paolo Nuciforo, Roberta Fasani, Vicente Peg, Isabel Rubio, Javier Cortés, Violeta Serra, Santiago Escriva-de-Romani, Jeff Sperinde, Ahmed Chenna, Weidong Huang, John Winslow, Joan Albanell, Joan Seoane, Maurizio Scaltriti, Jose Baselga, Josep Tabernero, Pablo Umana, Marina Bacac, Cristina Saura, Christian Klein, Joaquín Arribas*

*Corresponding author. Email: jarribas@vhio.net

Published 3 October 2018, *Sci. Transl. Med.* **10**, eaat1445 (2018)
DOI: 10.1126/scitranslmed.aat1445

The PDF file includes:

Other Supplementary Material for this manuscript includes the following:

(available at www.sciencetranslationalmedicine.org/cgi/content/full/10/461/eaat1445/DC1)

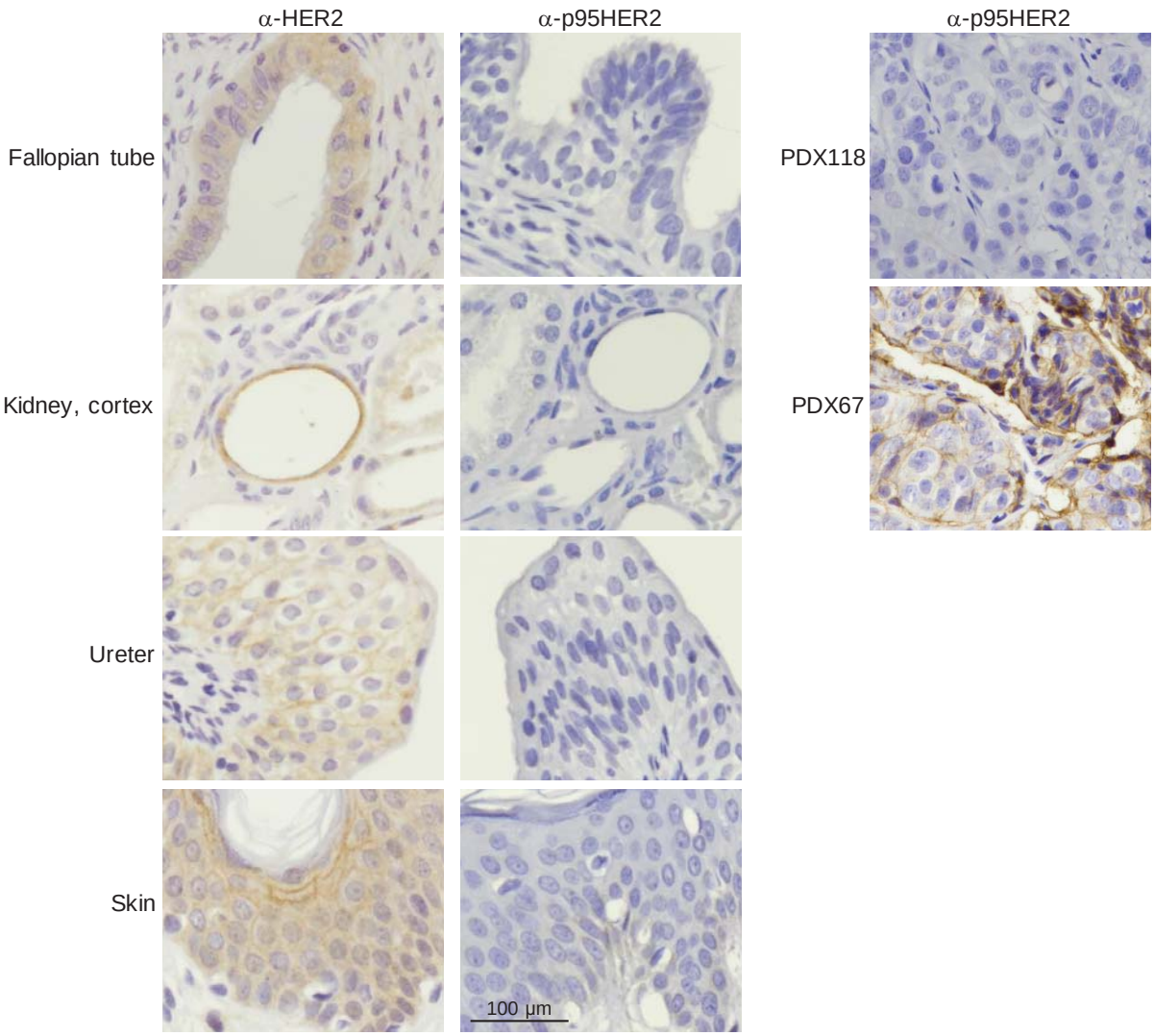

Figure S1. Expression of p95HER2 in normal tissues.

Immunohistochemical analyses of the expression of HER2 and p95HER2 in selected normal tissues. As controls, we stained samples from PDX118 and PDX67, in parallel and under the same conditions. These samples are negative and positive for p95HER2, respectively.

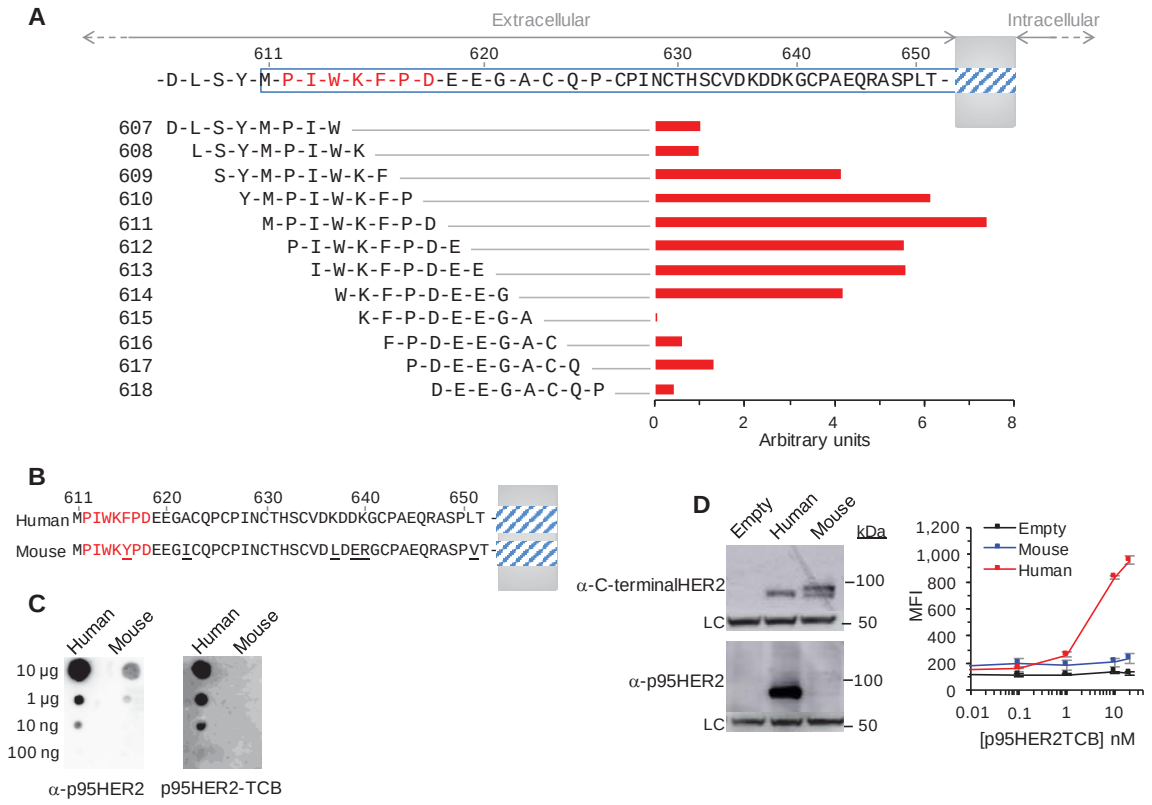

Figure S2. Identification and characterization of the epitope recognized by the monoclonal antibody used to generate p95HER2-TCB.

A, upper, schematic showing the amino acid sequence of the juxtamembrane extracellular region of HER2. p95HER2 starts at methionine 611. The epitope recognized by α-p95HER2, the antibody used to generate the p95HER2-TCB antibody, is shown in red.

Lower panel, overlapping 8-mer peptides were synthesized, immobilized and incubated with the α -p95HER2 and an anti-mouse secondary antibody coupled to peroxidase. Blots were developed and signals were quantified and expressed as arbitrary units.

B, sequences of HER2 and its murine homolog. Differences in the amino acid sequence are underlined.

C, PIWKFPD and PIWKYPD peptides, corresponding to the human and mouse sequences, respectively, were synthesized, immobilized, and incubated with α-p95HER2 or with the p95HER2-TCB. Then, blots were incubated with an anti-mouse secondary antibody coupled to peroxidase and developed.

D, HEK293 cells were transfected with empty vector or the same vector encoding mouse or human p95HER2. Expression of p95HER2 was analyzed by Western blot with an antibody against the C-terminus of HER2, which recognizes an epitope conserved in human and mouse, or α-p95HER2 (left panels). β-tubulin staining is shown as loading control. Flow cytometry analyses were also performed with the p95HER2-TCB antibody (right panel), n= 3 expressed as mean ± standard deviation (SD).

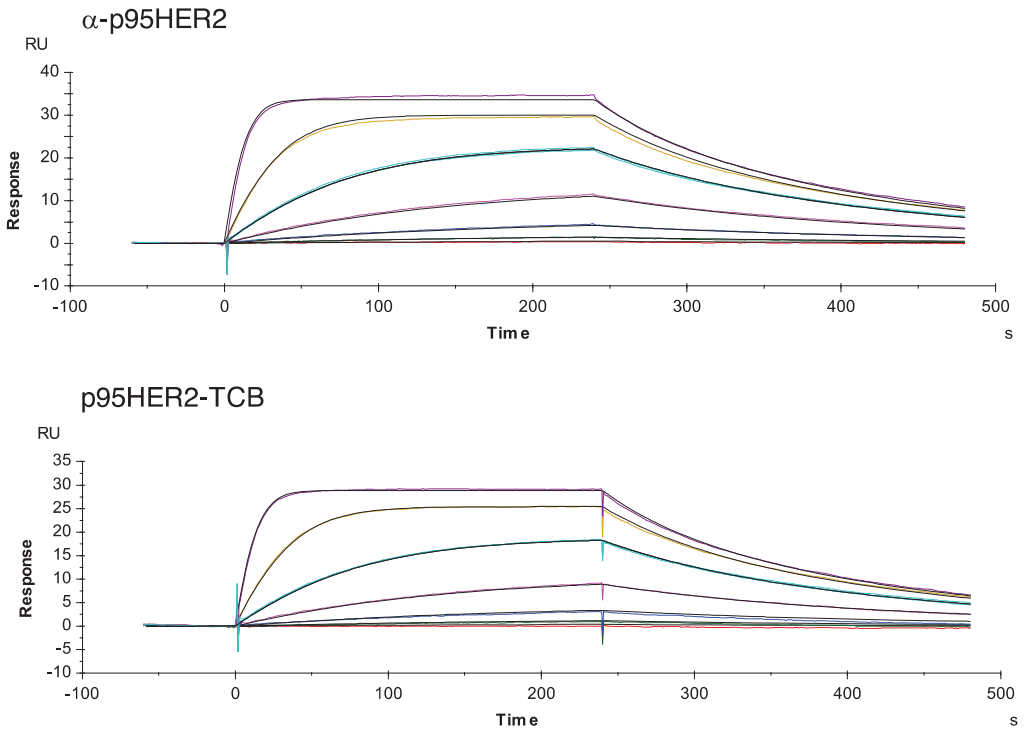

	ka (1/Ms)	kd (1/s)	KD (M)	KD	Rmax (RU)	Chi² (RU²)
anti-p95HER2	1.05E+06	8.45E-03	8.02E-09	8 nM	35.9	0.13
	1.10E+06	9.80E-03	8.92E-09	9 nM	58.2	4.07
p95HER2-TCB	1.02E+06	9.08E-03	8.91E-09	9 nM	30.9	0.13
	1.00E+06	9.14E-03	9.12E-09	9 nM	49.8	5.47

Figure S3. Affinities of the original anti-p95HER2 monoclonal antibody and the p95HER2-TCB.

KD binding affinity of anti-p95HER2 and p95HER2-TCB to the p95HER2 peptide as detected by surface plasmon resonance. Kinetic evaluation was performed by global fitting of the data to a 1:1 interaction model. Results of two independent duplicates, one sensorgram shown for illustration.

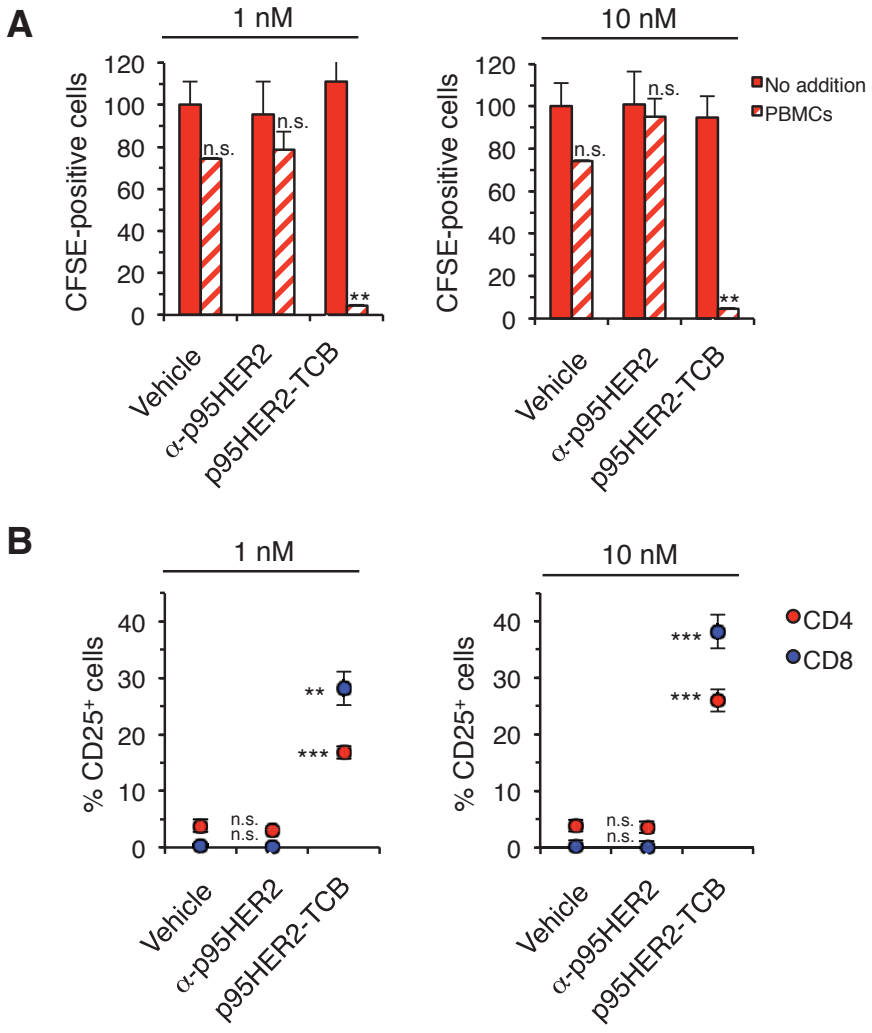

Figure S4. Effect of anti p95HER2 and HER2 TCB on cultures of MCF7 p95HER2 cells with or without PBMCs.

CFSE-labeled MCF7 p95HER2 cells were incubated with 1 nM (left) or 10 nM (right) of the indicated antibodies and without or with PBMCs for 48 hours. Then, CFSE-positive cells were counted by flow cytometry and normalized to cells treated with vehicle (A), and the percentages of $CD25^+$ cells were assessed on $CD8^+$ or $CD4^+$ subpopulations by flow cytometry (B), n= 3 expressed as means ± SD.

$^{**}P<0.01$, $^{***}P<0.001$, two-tailed *t* test

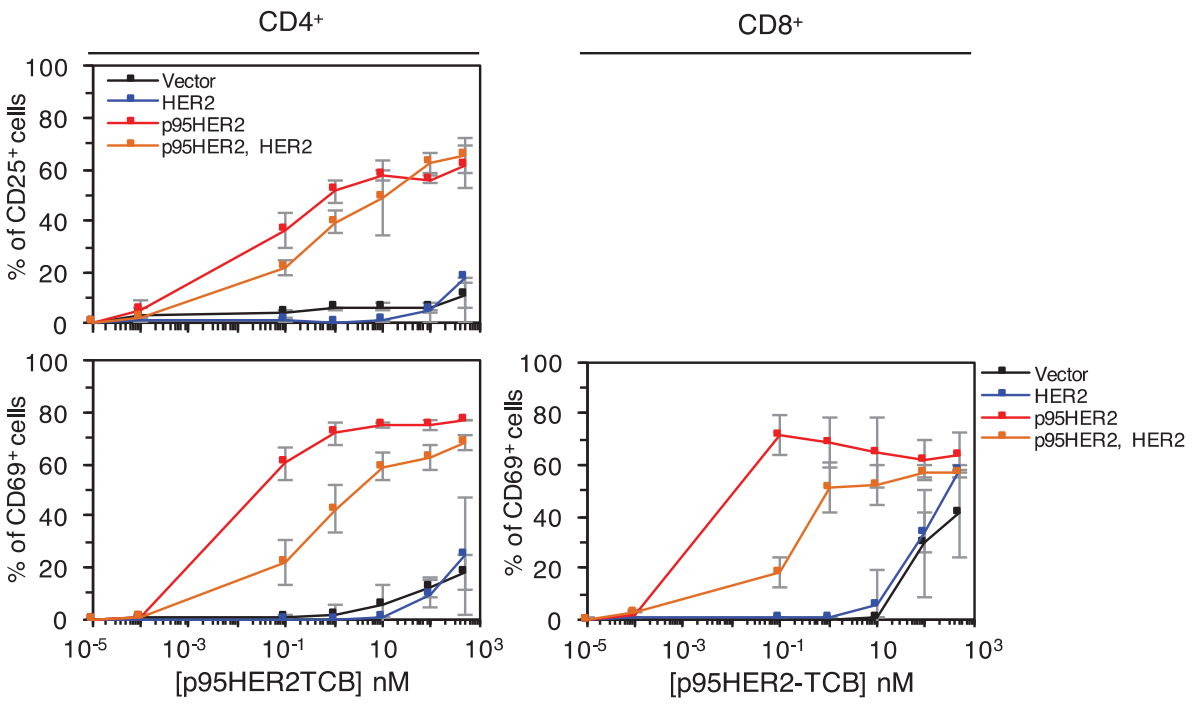

Figure S5. Effect of p95HER2-TCB on the activation of CD4⁺ and CD8⁺ cells in cocultures of MCF10A cells transfected with HER2 and/or p95HER2 and PBMCs.

MCF10A cells transfected with the indicated vectors were incubated with PBMCs and different concentrations of p95HER2-TCB for 48 hours. Then, the expression of the activation markers CD25 and CD69 was assessed on CD4⁺ and CD8⁺ cells by flow cytometry, n= 3 expressed as means ± SD.

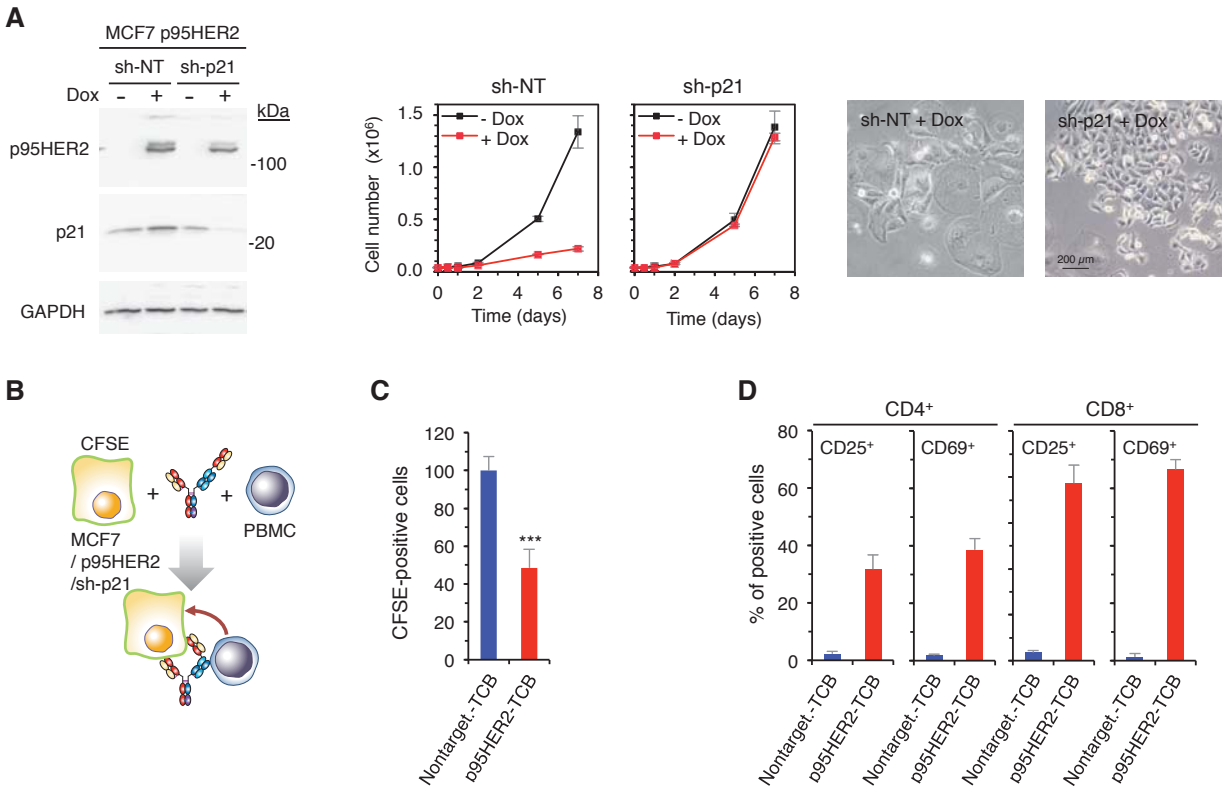

Figure S6. Generation of proliferating MCF7 cells expressing p95HER2.

A, MCF7 Tet-On p95HER2 cells were transfected with vectors encoding control shRNAs (sh-NT) or a shRNA targeting p21 (sh-p21). Expression of p95HER2 in control MCF7 cells causes oncogene-induced senescence *(25)*, and thus, to the inhibition of cell proliferation and a profound morphological change (sh-NT +Dox). Downmodulation of p21 overcomes senescence, resulting in normally proliferating MCF7 cells expressing p95HER2 (sh-p21), n= 3 expressed as means ± SD.

B, Schematic drawing illustrating the co-culture experiments. To follow their fate, MCF7 p95HER2 sh-p21 cells were labeled with the fluorochrome CFSE.

C, CFSE-labeled MCF7 p95HER2 sh-p21 cells were incubated with PBMCs and control non-targeting TCB or p95HER2-TCB for 48 hours. Then, CFSE-positive cells were counted by flow cytometry and normalized to non-targeting TCB. ***P<0.001, two-tailed t test.

D, Cells were treated as in C, and the expression of the activation markers CD25 and CD69 was assessed on $CD4^+$ and $CD8^+$ cells by flow cytometry.

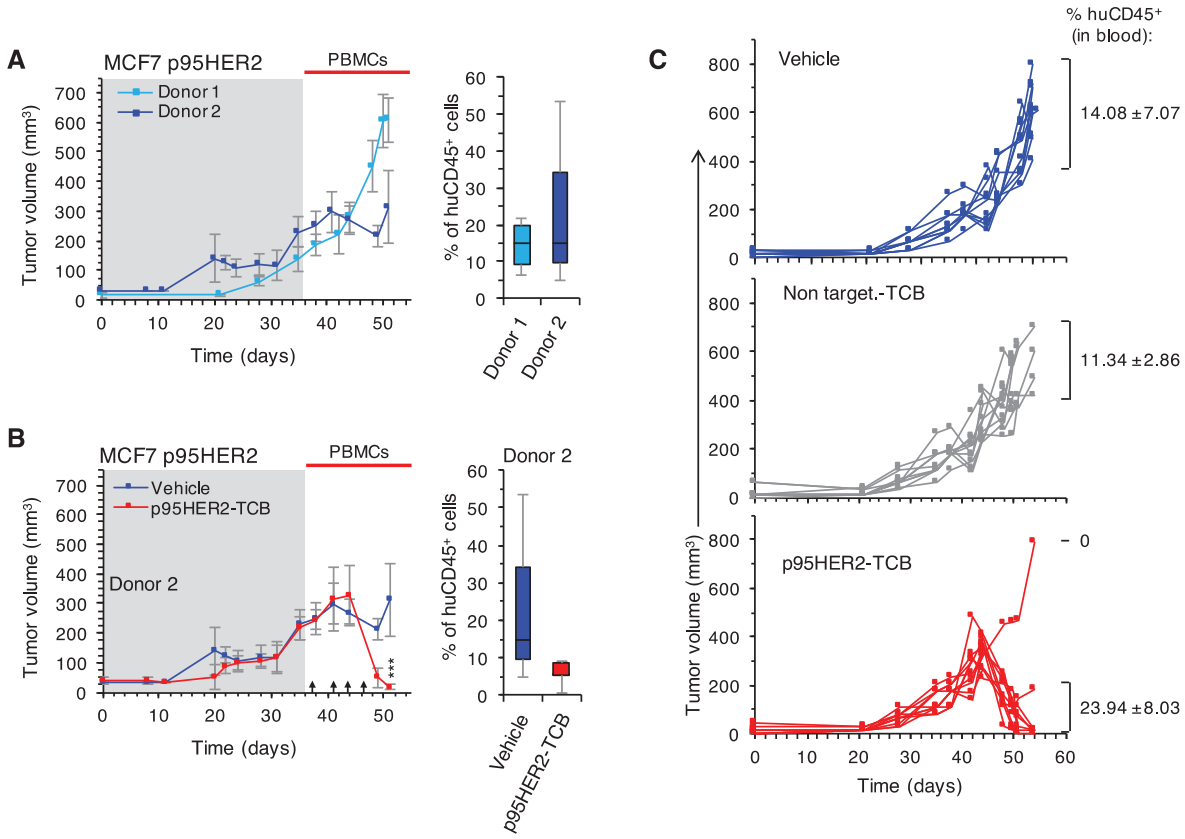

Figure S7. Effects of PBMCs from different donors and of p95HER2-TCB on the growth of MCF7 p95HER2 cells as xenografts.

A, left, Means ± SD are shown, n ≥ 5 per group. When tumors reached ~200 mm^3 (shadowed), human PBMCs from two healthy donors were transferred. Right, percentage of circulating human $CD45^+$ relative to total leukocytes, at the end of the experiment.

B, left, NSG mice humanized as in A. Means ± SD are shown (n ≥ 5 per group). Mice were treated with vehicle (control) or 1 mg/kg of p95HER2-TCB (arrows). Right, percentage of circulating human $CD45^+$ was measured as in A.

C, Growth curves of individual tumors shown in Fig. 3B. The percentages of circulating human $CD45^+$, relative to total leukocytes, at the end of the experiment are shown as means ± SD. Note that the only tumor that grew after treatment with p95HER2-TCB was implanted in a mouse with no detectable human $CD45^+$ circulating cells.

$^{**}P<0.01$, $^{***}P<0.001$, two-way ANOVA and Bonferroni correction.

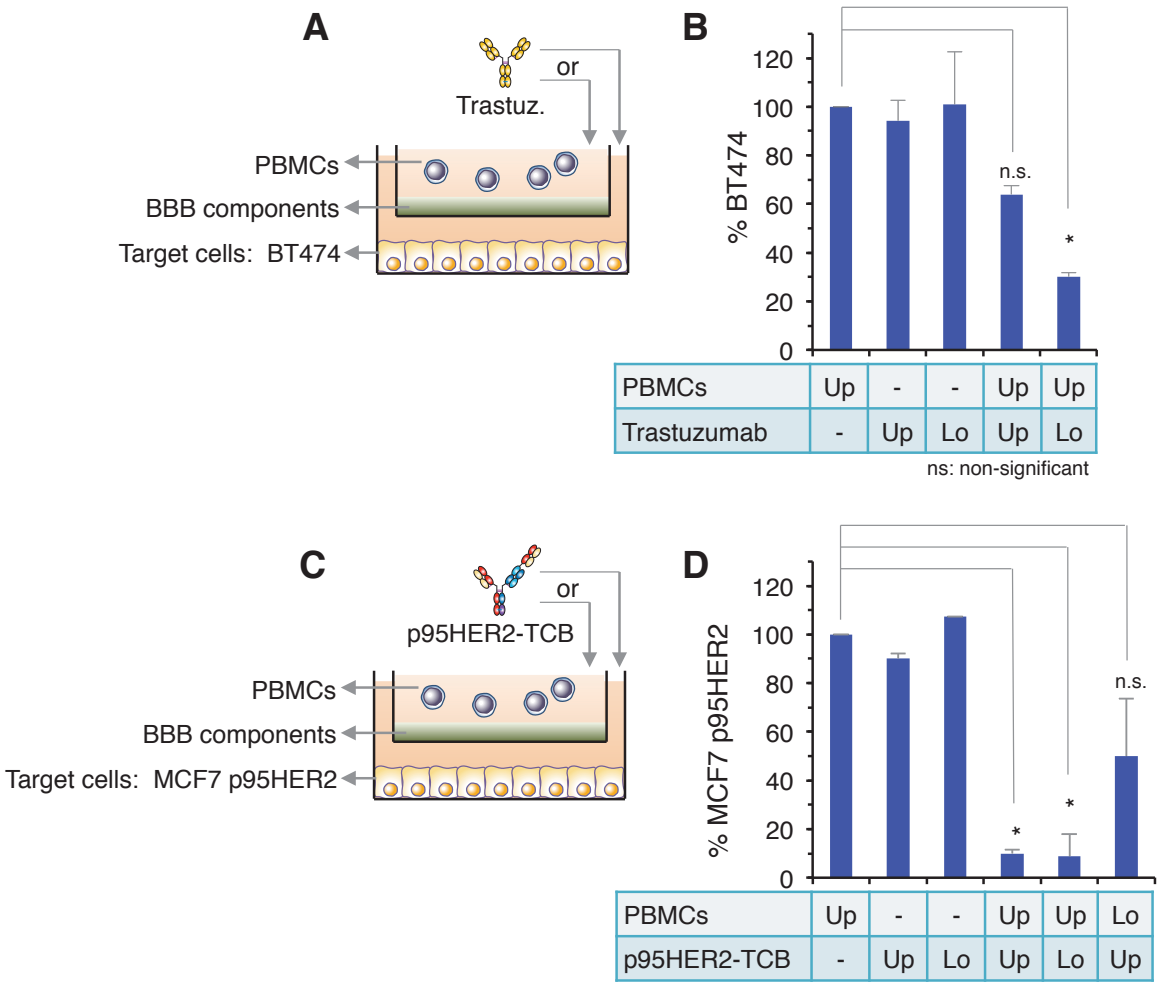

Figure S8. Effect of p95HER2-TCB on an in vitro model of BBB.

A, a BBB model was generated by seeding hCMEC/D3 cells in the upper chamber of transwells precoated with collagen and fibronectin. CFSE-labeled target BT474 cells were seeded in the lower chamber, PBMCs were added to the upper chamber, and trastuzumab was added to the upper or lower chambers as indicated. After incubation for 72 hours, BT474 cells were counted and means ± SD are presented in B.

C, D an experiment similar to that described in A was performed with MCF7 p95HER2 cells and p95HER2-TCB.

* $P<0.05$, two-tailed *t* test.

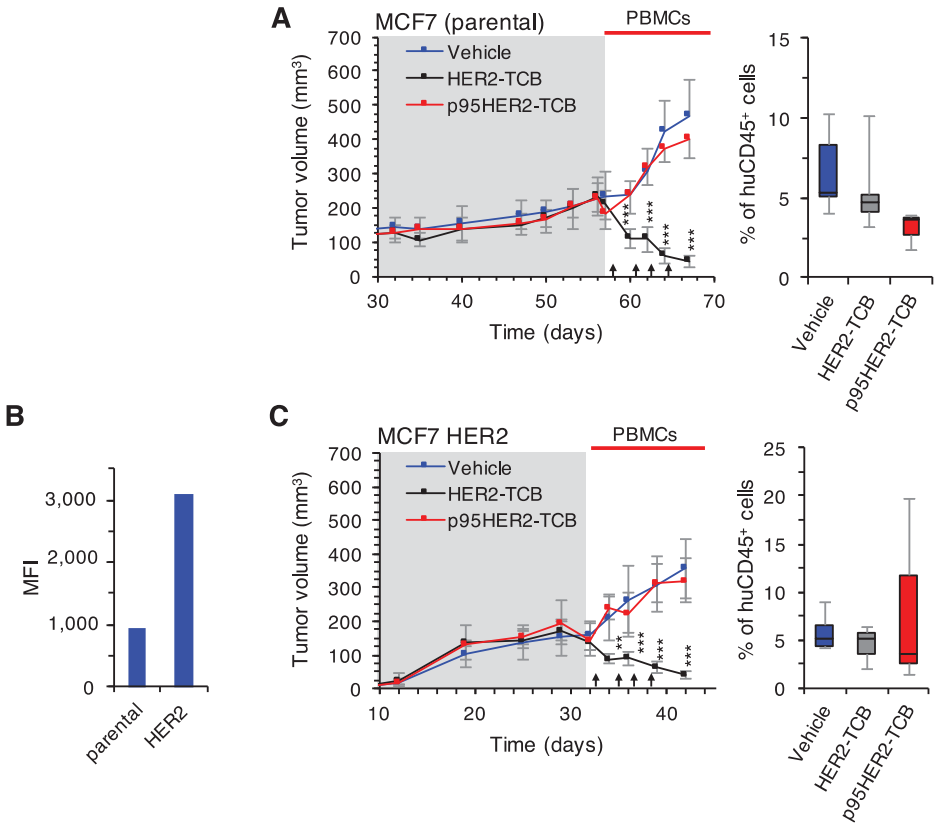

Figure S9. Effect of p95HER2-TCB on parental MCF7 cells and on MCF7 cells transfected with HER2.

A, left, NSG mice (n ≥ 6 per group) were injected with parental MCF7 cells and humanized with PBMCs. Mice were treated with vehicle (control), 1 mg/kg of HER2-TCB, or p95HER2-TCB (arrows). Right, percentage of circulating human CD45$^+$.

B, parental MCF7 cells or the same cells transfected with a vector encoding HER2 were analyzed by flow cytometry with trastuzumab.

C, left, NSG mice (n ≥ 6 per group) were injected with MCF7 HER2 cells, humanized, and treated as in A. Right, percentage of circulating human CD45$^+$.

**P<0.01, ***P<0.001, two-way ANOVA and Bonferroni correction.

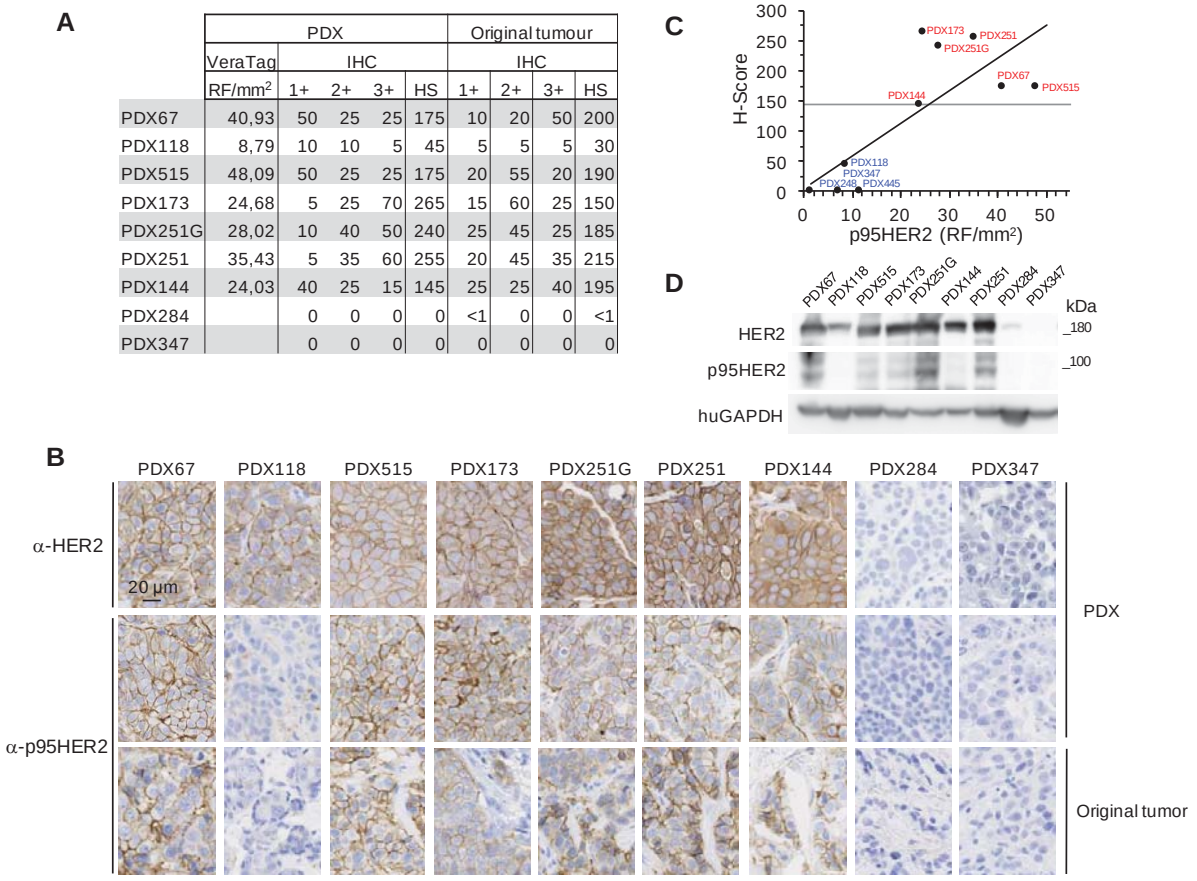

Figure S10. Expression of p95HER2 in different PDXs.

A, Expression of p95HER2 in PDXs and the corresponding original tumors determined by a quantitative IHC-based assay or H-score *(20)*. Numbers in the columns labeled “1+,” “2+,” and “3+” are the percentages of positive cells in each intensity category.

B, Representative IHC analysis of the samples in A.

C, H-scores were plotted against the amount of p95HER2 determined using a quantitative IHC-based assay (VeraTag). In red and blue are PDXs that scored positive and negative, respectively, for the activation of T cells mediated by p95HER2-TCB (Fig. 5).

D, Lysates from the indicated PDXs were analyzed by Western blot with antibodies against the c-terminus of HER2, and anti-human GAPDH was used as a loading control.

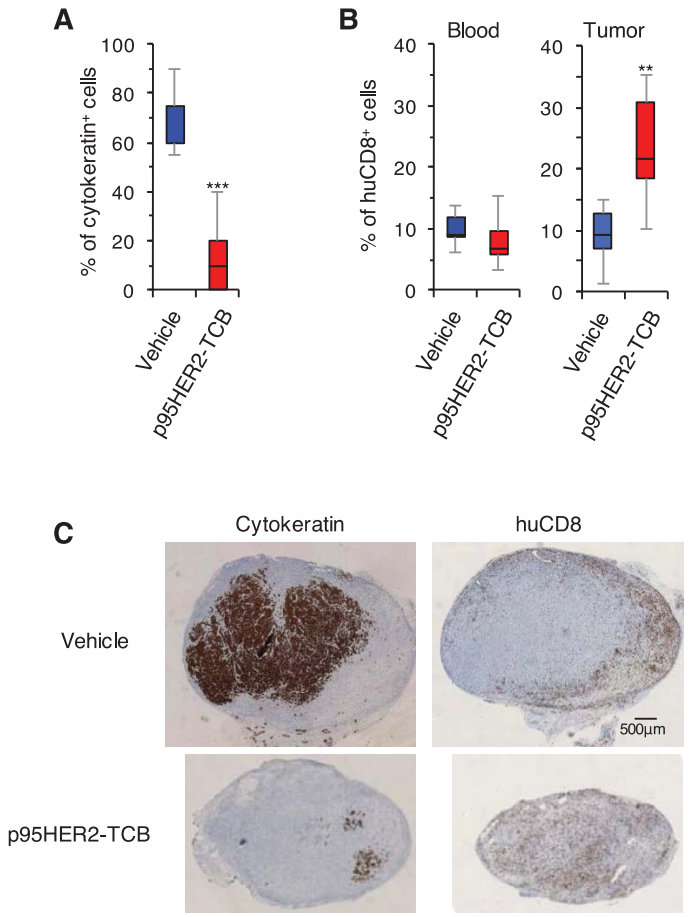

Figure S11. Cytokeratin expression and lymphocyte infiltration in PDXs treated with p95HER2-TCB in vivo.

A, Cells positive for cytokeratin were identified by immunohistochemistry and quantified.

B, Percentages of circulating (Blood) and intratumoral (Tumor) human $CD8^+$ cells at the end of the experiment shown in Fig. 6A (non-matched). Percentages in blood were calculated by flow cytometry and are relative to total leukocytes. Percentages in tumors were calculated by immunohistochemistry and are relative to tumor cells.

C, Representative IHC analyses corresponding to tumors analyzed as in A and B.

$^{**}P<0.01$, $^{***}P<0.001$, two-tailed *t* test.